AGGREGATION IN DODECYLTRIMETHYLAMMONIUM BROMIDE – DIDODECYLDIMETHYLAMMONIUM BROMIDE AQUEOUS MIXTURES

Proverbio, Z.E.[a]; Messina, P.V.[a]; Ruso, J.[b]; Prieto, G.[b]; Schulz, P.C.[a]*; Sarmiento, F.[b]

[a*] Departamento de Química, Universidad Nacional del Sur, Bahía Blanca, Argentina

Fax: +54 291 5495160, E-Mail: pschulz@criba.edu.ar

[b]Departamento de Física Aplicada, Facultade de Física, Universidade de Santiago de Compostela, Santiago de Compostela, Spain

Received March 20th, 2006. In final form, September 21st, 2006

Abstract

The characteristics of the aggregation of the aqueous mixed system dodecyltrimethylammonium bromide - didodecyldimethylammonium bromide were studied by several techniques. The mixed systems show a coexistence of small spherical micelles, and a polydisperse mixture of vesicles and aggregates of micelles. The charge and size of aggregates were studied as a function of the mixture composition.

Resumen

La agregación de mezclas acuosas de bromuro de dodeciltrimetilammonio y bromuro de didodecildimetilamonio fue estudiada mediante varias técnicas. Se observa la coexistencia de pequeñas micelas esféricas y una mezcla polidispersa de vesículas y agregados de micelas. La carga y tamaño de los agregados fue estudiada en función de la composición de la mezcla.

Introduction

Micelle formation of mixtures of surfactants is of considerable interest from both fundamental and practical points of view. Surfactants used in practical applications are often mixtures of homologous compounds or are contaminated by impurities. In addition, mixed aggregates of two or more components are important in biological systems. Much of the work in the biochemical literature has focused on mixed micelles of monoalkyl surfactants and phospholipids [1-3]. Mixed aqueous dispersions of lipids and surfactants have been considered as potential tools for membrane research and protein reconstitution. The initial compositions of lipid-surfactant mixtures and the changes in local compositions of the mixtures during surfactant removal are very important in forming stable lamellar structures in the formation of vesicles and in protein reconstitution processes [4-9].

Although both hydrocarbon tail length and headgroup effects have been extensively studied for surfactant mixtures, little work has been devoted to monoalkyl / dialkyl surfactant mixtures, in

which the volume occupied by the hydrocarbon tails is the parameter varied through compositional changes. Most of the work concerning monoalkyl / dialkyl surfactant mixtures has appeared in the biochemical literature [1-3, 10], where the effects of monoalkyl surfactants on phospholipid bilayers have been extensively studied. These effects include fluidification of bilayers [1], break down of cell membranes [3,10] and suppression of the immune response in animals [11].

Monolayer curvature is determined by several factors including geometric constraints, repulsive forces between neighbouring headgroups, and the chain – packing of hydrocarbon tails [12]. Manipulating the monolayer composition modifies the factors determining the curvature and aggregate size so that the aggregate composition can be efficiently and systematically changed. As shown by simple packing arguments, changes in average geometric parameters per surfactant molecule, such as headgroup area, tail length, or tail volume, significantly modify the geometry of the surfactant aggregate [12,13]. It may be supposed that altering the didodecyldimethylammonium bromide (DDAB)-dodecyltrimethylammonium bromide (DTAB) mixing ratio provides a means for studying structural changes induced by changes of the average tail volume per molecule, since headgroup areas and tail lengths are nearly equivalent for DTAB and DDAB. This leads to the assumption of ideal mixing. However, data in literature are contradictory, ideal behaviour was reported for DDAB-DTAB mixtures [14], whereas nonideal properties were informed for DDAB-dodecyltrimethylammonium chloride (DTAC) [15,16].

In this work we continued the study of the DDAB - DTAB system, which shows a nonideal interaction as it was found in a previous paper [16].

Experimental

Dodecyltrymethylammonium Bromide (DTAB) and Didodecyldimethylammonium Bromide (DDAB) of analytical grade were purchased from Sigma. Doubly distilled water was used. For each surfactant mixture composition, a concentrated aqueous solution was prepared by weighing both surfactants, and then adding water to the desired volume. Mixtures with total mole fraction of DDAB (without taking into account water) α_{DDAB} = 1, 0.875, 0.75, 0.625, 0.5, 0.375, 0.25, 0.125, 0.05 and 0 were prepared. Working solutions were made by dilution of the concentrate.

To perform light scattering and zeta potential measurements, solutions for each α_{DDAB} value were prepared with concentrations equal to 1.3CAC, 1.6CAC, 2CAC and 3 CAC. The CAC is defined as the concentration at which aggregates (vesicles and /or micelles) appear for each mixture composition (α_{DDAB}). The CAC values were determined in a previous work [16] and are shown in Table I.

Light scattering measurements were made on a Zetasizer 2700 from Malvern Instruments England, at 90º and 25 ºC, λ = 488.0 nm, intensity 3.96, dispersant RI = 1.331.

Zeta potentials were obtained with a Zetamaster Model 5002 by taking the average of (at least) five measurements at stationary level. The cell used was a 5 mm × 2 mm rectangular quartz capillary. Other conditions were; T = 25 ºC, angle 90º, RI dispersant 1.331, dielectric constant 79.0.

To produce the uranyl staining of the different samples, one milliliter of each solution (with different α_{DDAB} and C = 2 or 4 times the critical aggregation concentration, CAC) was mixed with 1 mL of 2 % aqueous uranyl acetate and sonicated for ca. 20 s in an ultrasonic bath. The mixture then was incubated in an ice-water bath for 30 minutes and applied to a carbon-coated Cu grid and dried under vacuum. A JEOL 100 CX II transmission electron microscope was used

for the measurement, operating at 100 kV with a magnification of 100,000X. When micelles were detected, their diameter was measured with a comparison microscope having a measuring precision of 0.02 mm.

Ion-selective measurements were made with a CRIBABB millivoltmeter with an Orion Br^--ion-selective electrode and a dodecyltrimethylammonium (DTA^+) ion-selective electrode. Both electrodes were measured against a saturated calomel electrode. The fabrication of the DTA^+ ion-selective electrode was described elsewhere [17].

Conductivity measurements were performed with an immersion cell and an automatic conductimeter, Antares II of Instrumentalia. The device was calibrated with a KCl solution. Measurements were made twice by titration of 50 ml water with each concentrated solution. Each addition of the concentrated surfactant mixture was followed by shaking and subsequent determination of the conductivity.

All determinations were made at 25.0 ºC.

Mean values and variances were computed by the minimum variance linear unbiased method [18] and the Student *t* function was employed to compute the error intervals. Confidence level was 0.90. Errors of derived data were computed with the error expansion method.

Table 1. *Critical aggregation concentration and micelle composition (X_{DDAB}) of DDAB-DTAB mixtures from reference [16].*

α_{DDAB}	1	0.875	0.75	0.625	0.5	0.375	0.25	0.125	0 _
CAC/ mol.dm^{-3}	5.34x10^{-5}	0.00027	0.00032	0.00025	0.000233	0.000338	0.00123	0.00265	0.01517
Error ±	0.33x10^{-5}	-	0.00003	-	0.000066	0.000063	0.00023	0.00035	0.00033
X_{DDAB}	1	0.997	0.995	0.993	0.993	0.9869	0.940	0.848	0

Results and Discussion

The charge of aggregates

Figure 1 shows the ζ potential at the critical aggregation concentration (CAC) as a function of α_{DDAB}. The CAC was determined in a previous work [16] for each surfactant mixture, and is shown in Table I together with the aggregates' composition (X_{DDAB}, the mole fraction of DDAB in aggregates). Mixed systems having low content of DDAB show a strong increase in the ζ potential with respect to the pure DTAB aggregates, while that of the systems rich in DDAB have a ζ potential smaller than that of pure DDAB aggregates. This behavior indicates a difference in the Stern layer structure of aggregates below and above $\alpha_{DDAB} \approx 0.5$, which in turn may indicate a difference in the structure of aggregates.

Figure 2 shows the ζ potential as a function of the aggregates' composition. It can be seen that the inclusion of very few DTAB molecules in the aggregates produces a sudden fall in the potential, which may be caused by an increase in the head groups layer compactness, accompanied by the capture of counterions. The inclusion of more DTAB molecules causes an increase in ζ up to a maximum at $X_{DDAB} = 0.94$ ($\alpha_{DDAB} = 0.25$). Then the ζ potential diminishes slowly. The change in the slope may mean that the structure of aggregates changes when $X_{DDAB} < 0.94$.

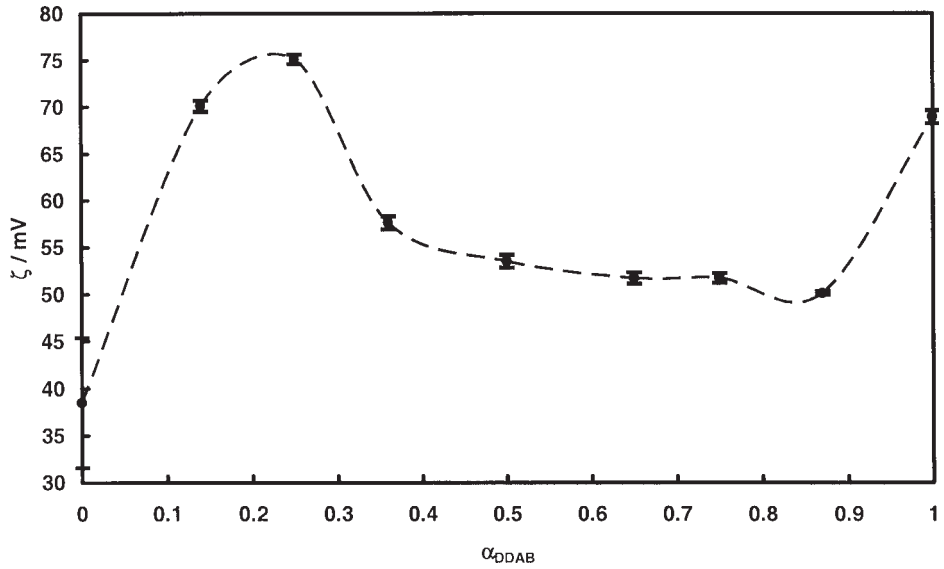

Figure 1. *ζ potential at the CAC of each surfactant mixture as a function of the system composition. The line is an eye guide.*

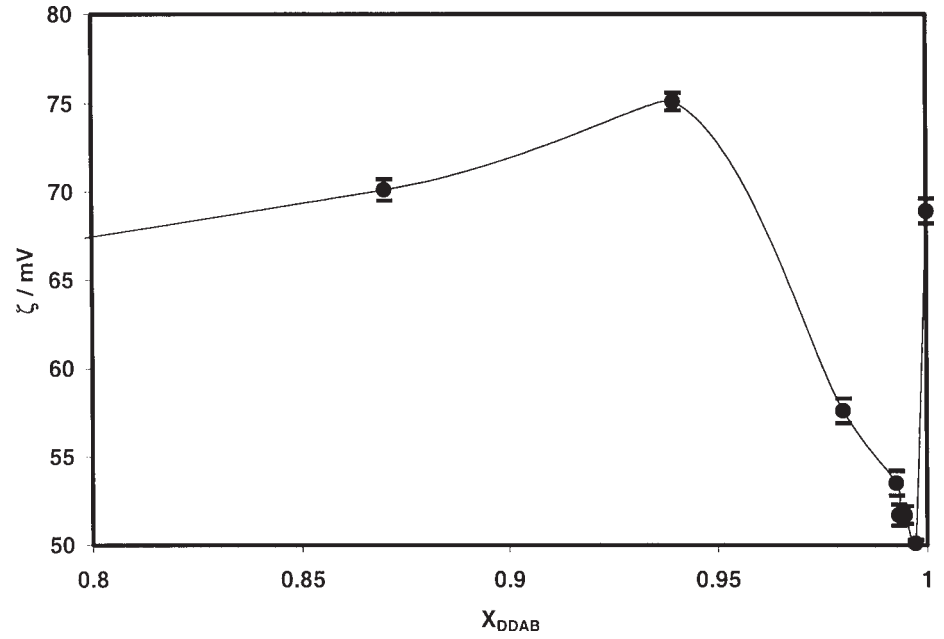

Figure 2. *ζ potential at the CAC of each surfactant mixture as a function of the aggregates' composition. The line is an eye guide.*

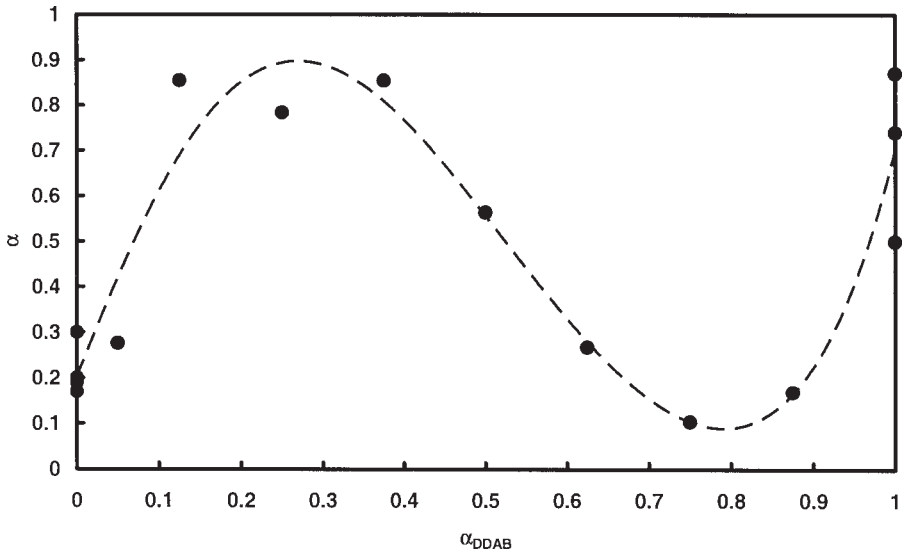

***Figure 3**. Ionization degree of aggregates determined from conductivity data, as a function of α_{DDAB}. The line is an eye guide.*

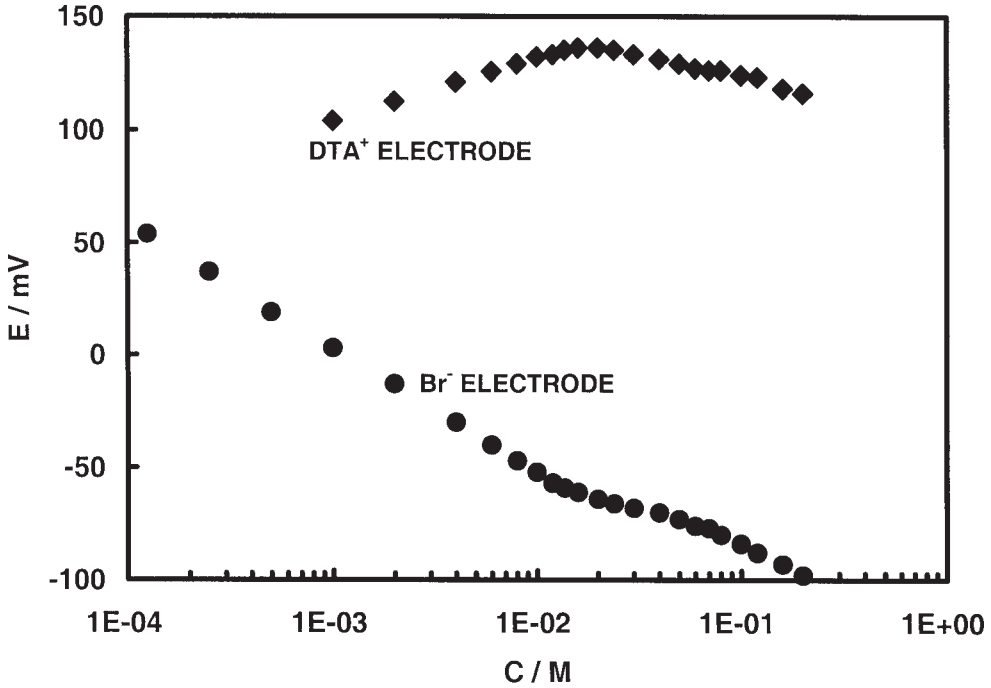

***Figure 4.** The response of the ion – selective electrodes as a function of the total concentration in the system α_{DDAB} = 0.5.*

The specific conductivity (κ) vs. concentration plots (not shown) was comprised of two right lines as usual. The ionization degree of mixed aggregates was computed as $\alpha = S_M/S_m$, where S_M and S_m are the slopes of the κ vs. C curve in the aggregates and monomeric zone,

respectively. This α value takes into account all the counterions released by aggregates. Figure 3 shows the ionization degree of aggregates (α) as determined from conductivity data, vs. the system composition (α_{DDAB}). It may be seen that the dependence of α on α_{DDAB} agrees with what may be expected on the basis of the ζ potential behavior. Since both properties were determined from measurements and theories having different theoretical backgrounds, these results support each other. The dependence of α on X_{DDAB} is similar to that of ζ vs. X_{DDAB} in Figure 2 and is not shown.

To control the α values obtained by conductivity, some measurements with ion-selective electrodes (Br^- and DTA^+) were run. Figure 4 shows the response of both electrodes as a function of the concentration for a sample with $\alpha_{DDAB} = 0.5$ (i.e, the middle of the composition range). The other systems with different α_{DDAB} values show an aggregation of bromide ions that agrees with the findings in conductivity and zeta potential measurements. Figure 5 shows the concentration of free (unaggregated) Br^- and surfactant, and that of aggregated surfactant (on a monomer basis) as a function of the total surfactant concentration, which were computed by a standard method [17]. Since the surfactant ion-selective electrode does not discriminate between DDA^+ and DTA^+ ions, it is not possible to know the separate concentrations of both free cationic surfactant ions.

Figure 6 depicts the dependence of the ionization degree of aggregates with $\alpha_{DDAB} = 0.5$ as a function of the surfactant concentration, obtained from the results of the ion-selective electrodes. As expected, α decreases as the concentration increases. Values for the pure surfactant solutions were taken from literature (DTAB: $\alpha = 0.17$ [19-23]; 0.19 [24]; 0.30 [25]; 0.19-0.20 [26]; DDAB : 0.74 – 0.87 [27], 0.5 [28]). It may be seen that the ionization degree at the CAC agrees with that obtained by conductivity.

The size and shape of aggregates

Figure 7 shows the diameter of the different species which are present in the systems as a function of α_{DDAB}. The diameter of micelles was measured on the TEM photomicrographs, whilst that of larger aggregates was measured by light scattering. The dashed line indicates the predominant component (i.e., that which involves the majority of the surfactant). Pure DTAB micelles have a diameter $d = 1.8 \pm 0.6$ nm. The aqueous DDAB solutions show polydispersity. While at the critical aggregation concentration almost the 100 % of the twin-tailed surfactant forms aggregates having 27.8 nm diameter, at higher concentrations there are larger aggregates. Matsumoto et al. [29] found vesicles having diameter of 10-22 nm, which also were detected by Kunitake et al.[30,31]. These vesicles increase in size between 3.6×10^{-4} mol.dm^{-3} and 6×10^{-4} mol.dm^{-3}, reaching a diameter of 100 - 215 nm, the same authors have detected large multilamellar liposomes at higher concentrations (2×10^{-3} mol.dm^{-3}) with diameters of several micrometers. Low concentration vesicles were probably monolamellar, whilst the larger liposomes have several concentric lamellae [32,33]. Mixtures show polydispersity.

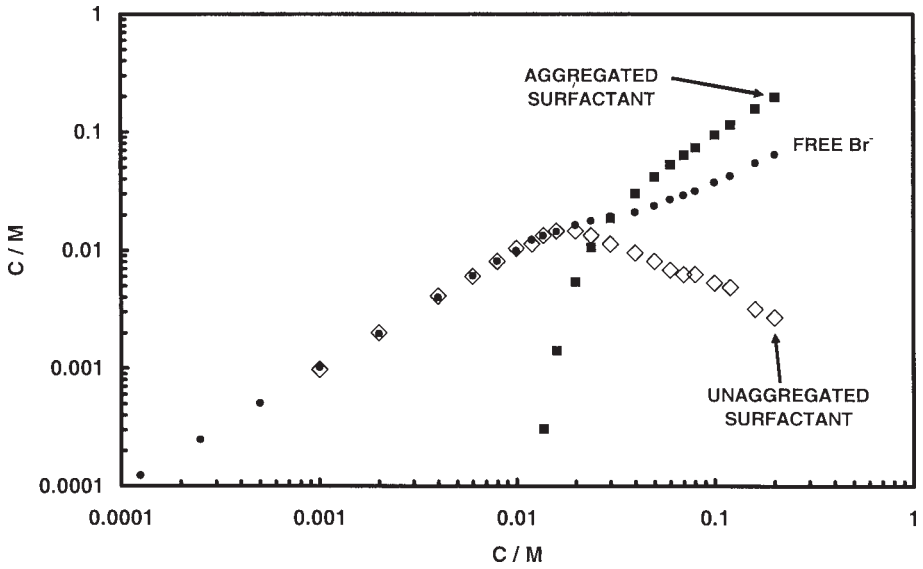

Figure 5. *Concentration of the different species vs. the total surfactant concentration in the system* α_{DDAB} *= 0.05.*

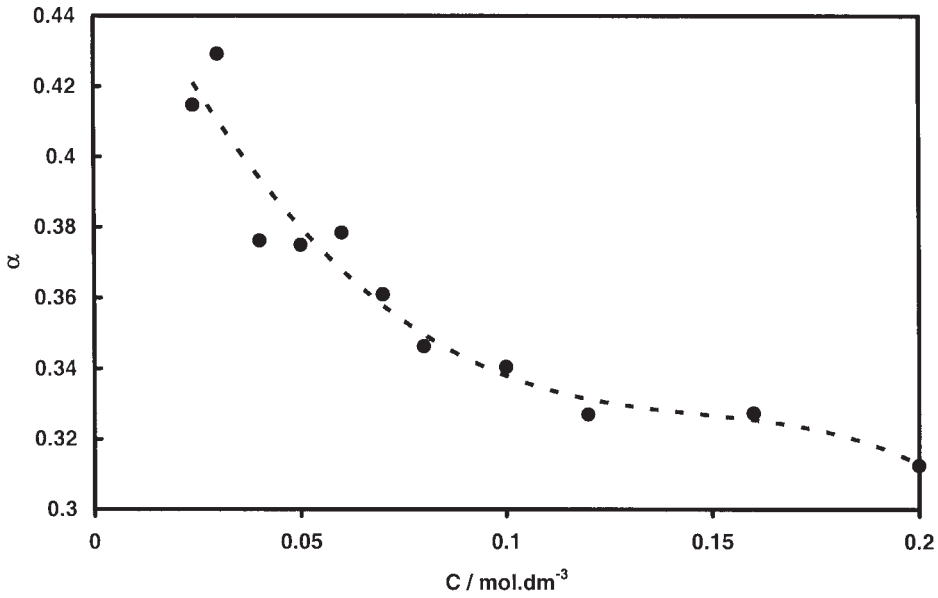

Figure 6. *Ionization degree of the aggregates as a function of the concentration determined by conductivity in the system* α_{DDAB} *= 0.5. The line is an eye guide.*

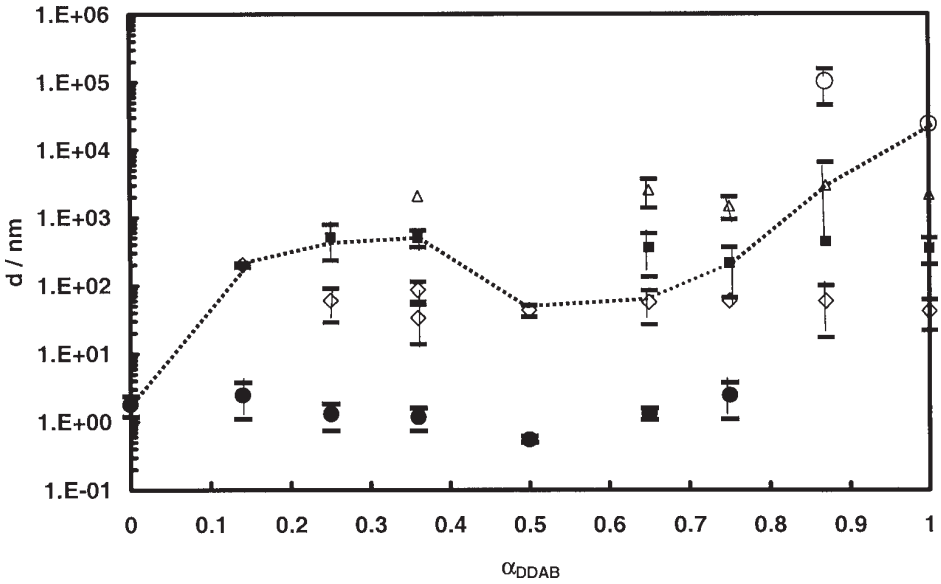

Figure 7*. Diameter of the different species present in the systems as a function of* α_{DDAB}*. The dashed line indicates the component in higher proportion. In various mixed systems, multilamellar vesicles coexist with small micelles. Points (•) were measured on the TEM microphotographs and correspond to micelles, the other data were obtained from light scattering measurements.The symbols (◇, ■, △, ○) indicate the different peaks of size distribution of vesicles.*

The dashed line in Figure 7 shows that the behavior of the aggregates' size is different below and above $\alpha_{DDAB} \approx 0.5$. When other factors remain constant, it is expected that a higher ζ potential should produce a smaller aggregate because of the increase in the head group's repulsion. However, in this system the situation is not so simple. Steric effects must be also considered [16]. As a result Figure 7 is not strictly correlated with the variations of the ζ potential.

There is a controversy about the coexistence of micelles and vesicles in this kind of mixtures. Viseu et al. [15] studied DDAB – DTAC (Dodecyltrimethylammonium Chloride) aqueous mixtures and found only vesicles, at a DTAC proportion as high as $\alpha_{DTAC} = 0.95$. However, Weers and Scheuing ([14] studied DDAB-DTAB mixtures and found micelles. They suggested that as DDAB is added to DTAB micellar solutions, spherical micelles undergo a transition from spheres to disks and then to rods as a function of composition. In the light of our findings, it seems that vesicles and micelles coexist, at least in some of the mixtures. The diameter of the larger spherical micelle of DTAB (i.e., those having a radius equal to the fully extended DTAB molecule) must be about 3.6 nm. All the lower diameter aggregates in the system had $d < 3.64$ nm (see Figure 7), as measured from the TEM images which show spherical micelles (see below).

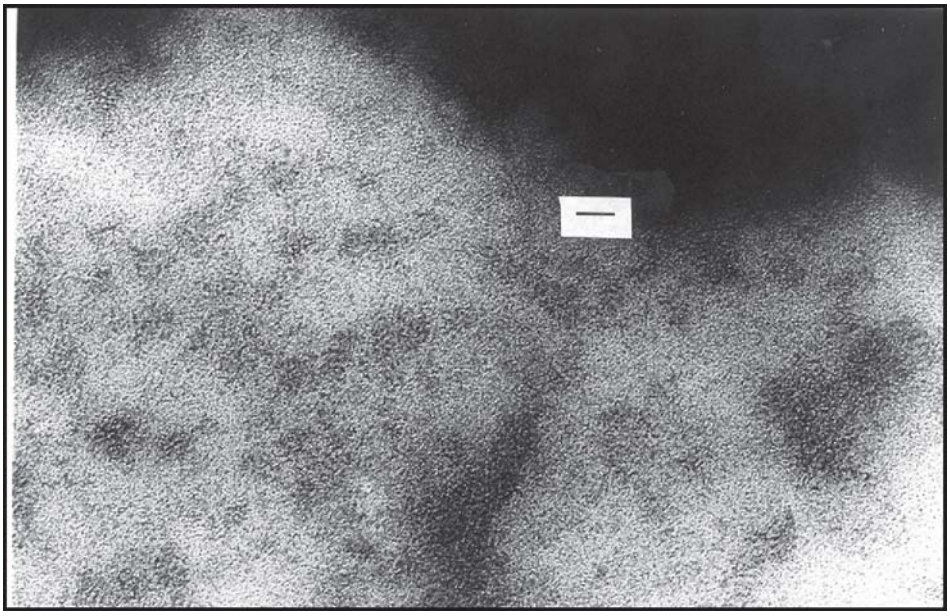

(a)

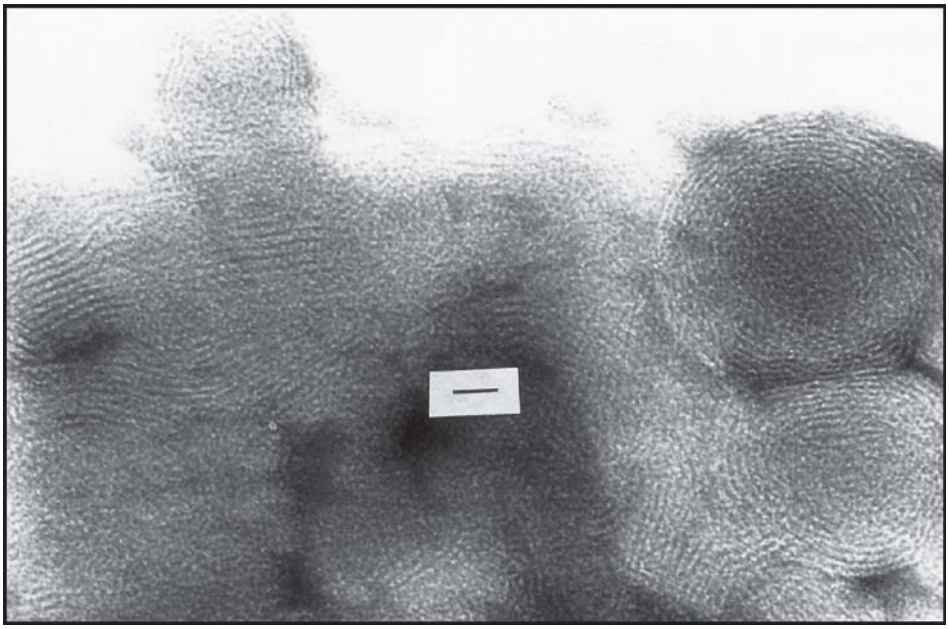

(b)

Figure 8*. TEM microphotographs of a: DTAB at twice the CMC, showing spherical micelles; b; DDAB at twice the CAC. Multilamellar vesicles and some small spherical micelles can be seen. The line represents 21 nm.*

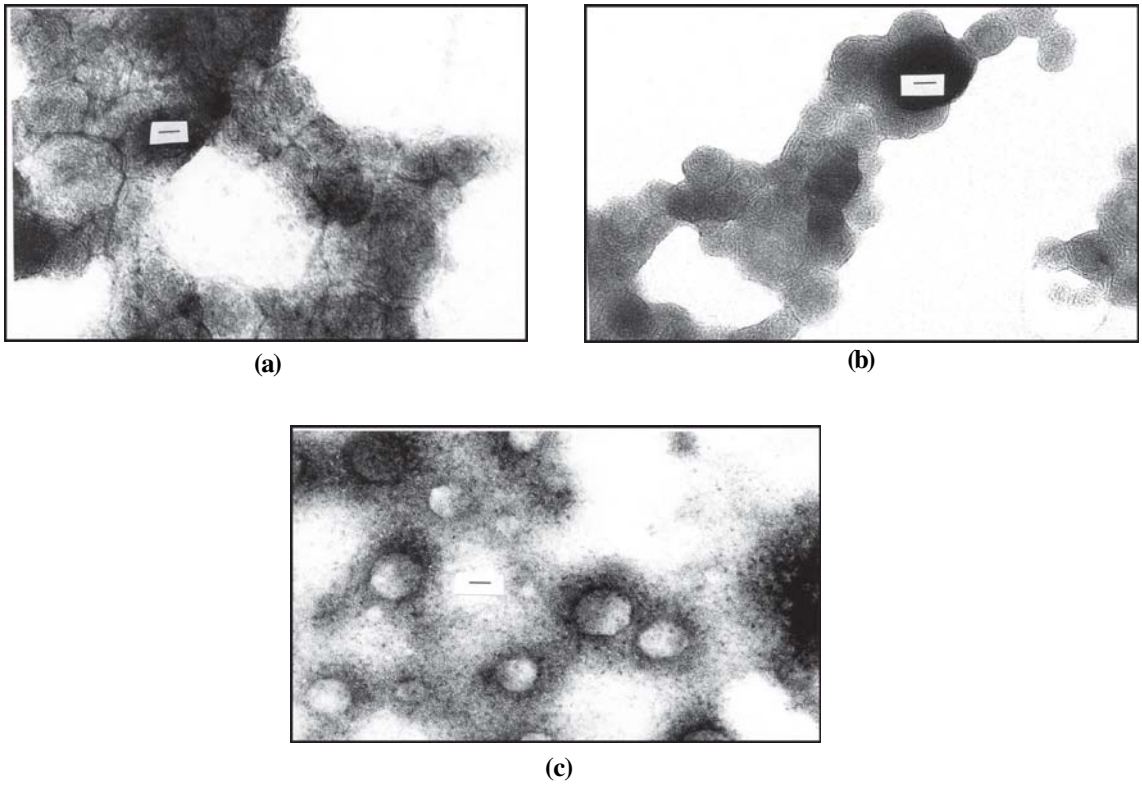

(a) **(b)**

(c)

***Figure 9**. TEM microphotographs of solutions of mixtures: **a** α_{DDAB} = 0.478 at C = 0.0005 mol.dm^{-3}; **b** and **c**; α_{DDAB} = 0.795 C = 0.00095 mol.dm^{-3}. Photo **a** mainly shows multilamellar vesicles, photo **b** shows multilamellar vesicles and photo **c** shows vesicles and small spherical micelles. The line represents 21 nm.*

To determine the nature of aggregates, TEM microphotographs were taken on some of the systems by the technique of negative uranyl staining. Figure 8 shows the TEM microphotographs of solutions of pure DTAB (a) at 2CMC with single spherical micelles and pure DDAB (b) at twice the critical aggregation concentration (CAC), showing multilamellar vesicles. Figure 9 shows the TEM microphotographs of solutions having α_{DDAB} = 0.478 and C = 0.0005 mol.dm^{-3} (a) and α_{DDAB} = 0.795 with C = 0.00095 mol.dm^{-3} (b and c). Photo of Figure 9a shows an agglomeration of polydisperse multilamellar liposomes with some spherical micelles. Photo 9b shows an agglomeration of not excessively polydisperse multilamellar liposomes. Photo 9c shows spherical micelles and spherical aggregates which may be unilamellar vesicles or agglomerations of spherical micelles. Samples with other α_{DDAB} values have shown similar images.

In conclusion, TEM microphotographs give support to the coexistence of micelles with vesicles, at most in some of the DDAB/DTAB proportions.

Concluding Remarks

- Mixed systems show a coexistence of small spherical micelles, and a polydisperse mixture of aggregates of micelles and vesicles.

- The charge and size of aggregates show a dependence on the total composition which is different below and above $\alpha_{DDAB} \approx 0.5$, this result may indicate a difference in the structure of aggregates. At $\alpha_{DDAB} \approx 0.25$ there is a maximum in ζ potential and α, corresponding to $X_{DDAB} = 0.94$.
- Both size and charge of aggregates are influenced by steric factors.

Acknowledgements

This work was supported by a grant of the Universidad Nacional del Sur and PIP # 2739 of CONICET, Argentina. Authors acknowledge financial support of the Spanish Ministerio de Educación y Ciencia, Plan Nacional de Investigación (I+D+i), MAT2005-02421. PVM, a CONICET fellow, thanks Banco Río for a grant to travel to Spain to work at the University of Santiago de Compostela.

References

[1] Sinensky, M.; Kleiner, J., *J. Cell. Physiol.* **1981,** *108*, 389.
[2] Lichtenberg, D.; Robson, R.J.; Dennis, D.A., *Biochim. Biophys. Acta*, **1983,** *737,* 285.
[3] Isomaa, B., *Ecol. Bull*. **1984,** *36*, 26.
[4] Mimms, L.T.; Zampighi, G.; Nozaki, Y.; Tanford, C., Reynolds, J.A., *Biochemistry,* **1982,** *20*, 833.
[5] Jackson, M.L.; Litman, B.J., *Biochemistry* **1982,** *21*, 5601.
[6] Uneno, M.; Tanford, C.; Reynolds, J.A., *Biochemistry,* **1984,** *23*, 3070.
[7] Schurtenberger, P.; Mazer, N.; Anzig, W., *J. Phys. Chem.* **1985,** *89*, 1042.
[8] Almong, S.; Lichtenberg, D., *Biochemistry,* **1988,** *27*, 873.
[9] Lévy, D.; Gulik, A.; Seigneurret, M.; Rigaud, J-L., *Biochemistry,* **1990,** *29,* 9480.
[10] Haydon, D.A.; Taylor, J., *J. Theoret. Biol.* **1963,** *4*, 281.
[11] Ashman, R.B.; Ninham, B.W., *Mol. Immunol.* **1985,** *22*, 609.
[12] Evans, D.F.; Mitchell, D.J.; Ninham, B.W., *J. Phys. Chem*. **1986,** *90*, 2817.
[13] Israelachvili, J.N.; Mitchell, D.J.; Ninham, B.W., *J. Chem. Soc. Faraday Trans. 1*, **1976,** *72*, 1525.
[14] Weers, J.G.; Scheuing, D.R., *J. Colloid Interface Sci.* **1991***, 145,* 563.
[15] Viseu, M.I.; Edwards, K.; Campos, C.S.; Costa, S.M.B., *Langmuir,* **2000,** *16*, 2105.
[16] Proverbio, Z.E.; Schulz, P.C.; Puig, J.E., *Colloid Polym. Sci*. **2002,** *280*, 1045.
[17] Schulz, P.C.; Morini, M.A.; Minardi, R.M.; Puig, J.E., *Colloid Polym Sci*. **1995,** *273*, 959.
[18]. Mandel, J., *Statistical Analysis of Experimental Data,* Interscience, New York, , **1964**. pp. 134-137.
[19] Derjaguin, B.V.; Landau, L., *Acta Physicochim. URSS,* **1941,** *14*, 633.
[20] Prins, W.; Hermans, J.S., *Konikl. Ned. Akad. Wetenschap, Proc*. **1956,** *B59*, 162.
[21] Mysels, K.J., *J. Colloid Sci.* **1955,** *10*, 507.
[22] Princen, L.H.; Mysels, K.J., *J. Colloid Sci.* **1957,** *12*, 594.
[23] Mysels, K.J.; Princen, L.H., *J. Phys. Chem.* **1959,** *63*, 1696.
[24] Scatchard, G.; Bergman, J., *J. Am. Chem. Soc*. **1959,** *81*, 6095.
[25] Stigter, D., *J. Phys. Chem*. **1960,** *64*, 842.

[26] Anacker, E.W.; Westwell, A.E., *J. Phys. Chem.* **1964,** *68*, 3490.
[27] Zana, R., *J. Colloid Interface Sci.* **1980,** *78*, 330.
[28] Soltero, J.F.A.; Bautista, F.; Pecina, E.; Puig, J.E.; Manero, O.; Proverbio, Z.; Schulz, P.C., *Colloid Polym. Sci.* **2000,** *278*, 37.
[29] Matsumoto, T.; Heiuchi, T.; Florie, K., *Colloid Polym. Sci.* **1989,** *267*, 71.
[30] Kunitake, T.; Okahata, Y., *J. Am. Chem. Soc.* **1977,** *99*, 3860.
[31] Kunitake, T., *J. Macromnol. Sci.* **1979,** *A13*, 583.
[32] Fontell, K.; Ceglie, A.; Lindman, B.; Ninham, B., *Acta Chem. Scand.* **1986,** *A40*, 247.
[33] Kacher, B.; Evans, D.F.; Ninham, B.W., *J. Colloid Interface Sci*. **1984,** *100*, 284.